

Article

Comparing Structural Casualties of the Ro-Ro Vessel Using Straight and Oblique Collision Incidents on the Car Deck

Aditya Rio Prabowo ^{1,*} , Dong Myung Bae ² and Jung Min Sohn ^{2,*}

¹ Department of Mechanical Engineering, Universitas Sebelas Maret, Surakarta 57126, Central Java, Indonesia

² Department of Naval Architecture and Marine Systems Engineering, Pukyong National University, Busan 48513, Korea; dmbae@pknu.ac.kr

* Correspondence: aditya@ft.uns.ac.id (A.R.P.); jminz@pknu.ac.kr (J.M.S.)

Received: 24 April 2019; Accepted: 6 June 2019; Published: 11 June 2019



Abstract: Roll on-roll off (Ro-Ro) ship is the preferable vessel for public transportation and also as a medium to distribute several commodities. Its operations are a straightforward process but traffic management is quite delicate, especially for cross-route. Moreover, maritime incidents sometimes occur, causing significant casualties and in the case of the Ro-Ro, collision with other ship is a possible threat with the ability to trigger immense damages. This research, therefore, was conducted to assess the structural casualties of a Ro-Ro vessel under collision. This was modelled with respect to a ship involved in a certain incident in Indonesia in the latest decade, and the designed collision problems were calculated using the finite element approach. The collision angle was selected as the main input parameter with the straight collision of angle 90° and oblique collision with different angles applied to the scenario. The results found the collision energy due to structural destruction to have distinct pattern and peak value under oblique cases with lower values observed for straight collision for all scenarios. It is, however, recommended that energy should be taken as an initial parameter in further investigation of structural damage and response contour.

Keywords: maritime incidents; straight and oblique collisions; finite element approach; energy ratio; rupture strain

1. Introduction

Transportation has been playing an important role in human society, and industrial development since the first industrial revolution took place more than two centuries ago. It started with the use of the animal as the driving force followed by the application of diesel engine in inland, aerospace, and water transportation. Furthermore, human interaction also experiences massive progress, for example, the use of a mobile phone makes it more convenient to communicate over long distances compared to the conventional methods of communication. This was followed by the evolution of these phones to become smart leading to easy business transactions, trading and several other forms of interaction. For the purpose of this study, transportation mode is focused because it requires carrying subjects from one location to the other based on designated missions, for example, it is possible to transport humans and commodities using a public vehicle which is classified as an inland transportation mode. However, most archipelago countries are faced with the challenges of obtaining another transportation mode to transport people on the island and this led to the use of water transportation mode by the public, thereby, making it become one of the highest maritime business potentials in these countries. Consequently, roll on-roll off (Ro-Ro) ship was considered the most suitable vessel in this situation due to its capability to convey a large number of vehicles, passengers, and commodities at the same time to cross the sea or strait.

The Ro-Ro ship is a vessel with the cargo wheeled or loaded/unloaded on board, in a vehicle or other platforms equipped with wheels. The first ships to be classified under this category were the Ferry equipped with railways to allow the transport of train carriages between the margins of the rivers considered too wide for bridges. The use of the Ro-Ro concept in merchant ships started in the late 1940s, early 1950's and mainly in the short-sea routes, such as inter-island route through the strait in archipelago countries. It became a significant vital transportation mode and a traffic connector. Furthermore, Figure 1 shows how the infrastructures for Ro-Ro spread on the islands of Indonesia thereby making domestic water traffic of the country to be very high. This is also influenced by the use of the strait between the islands as international route, especially from East Asian countries such as South Korea, Japan and China and Southeast Asia including Singapore to reach Australia [1–3].

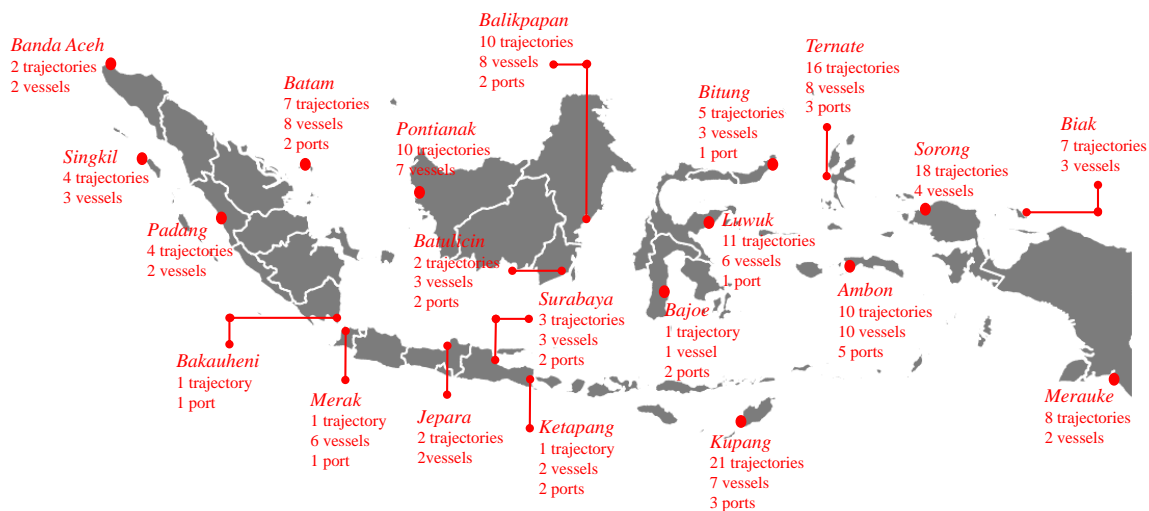


Figure 1. Location of port infrastructure across Indonesia territory (based on information in Ref. [4]).

With due consideration for the traffic situation of archipelago countries through the use of Indonesia as a representative, it is mandatory to ensure ship safety during daily operation. However, the most serious threat was observed to be the possible occurrence of impact load due to several causes, and the data recently released by Allianz [5] indicated collision and grounding to be the most frequent. The high number of casualties as a result of these usually vary, but they are all usually triggered by the structural rupture of the load [6–9], and this makes it important to conduct an analysis on the subject. Therefore, the objective of this study was to investigate the collision phenomenon of impact load involving two ships using a numerical approach, i.e., nonlinear finite element method (NLFEM). This method was considered suitable for this case since the analytical method is limited in term of material aspect and structural complexity and because the idealized phenomena were in large scale involving several parameters. Furthermore, the comparison of the structural parameters based on the NLFEM analysis was discussed as a contact scenario is designed by varying collision angle.

2. Literature Reviews: Ro-Ro and Maritime Incidents

The first time Ro-Ro was introduced to the public, it was intended to transport train carriages between the margins of the rivers considered too wide for bridges in Scotland and, for its effective operation, the vessel was equipped with railways. However, the war experienced across the European continent affected the rapid development of technology, water transportation inclusive. Moreover, the World War II motivated the improvement of Ro-Ro vessel to be more adaptable as landing vessel for military equipment and this is presently being used for both military and offshore industries as the Landing Craft Tank (LCT). After the war, the previously modified Ro-Ro was converted for other operation schemes like merchant ship MV Virginia Beach. Furthermore, in order to fulfill several objectives in maritime industries, Ro-Ro vessel was modified to provide several other types such as:

- **Ro-Ro passenger (Ro-Pax)** It has a large deck, and limited passenger facilities (less than passenger ferries) and its superstructures cover part of the deck.
- **Pure car carriers** It is designed for only one purpose, which is to efficiently transport cars or other types of vehicles such as bus, truck, etc. According to Wäertsillä, the largest deep-sea car carriers in service has the ability to convey up to 8000 car equivalent units [10].
- **Lift on-lift off (Lo-Lo)** This is similar to freight, but it has a different mechanism compared to general container vessel. The container vessel usually performed their loading and unloading with a port/harbor facility, while Lo-Lo conducts the process with the use of an onboard crane.

Identification of loss and risk during a vessel operation is very important in maritime industries, especially to a company’s financial and insurance policy and misconduct in this aspect has the ability to lead a company to bankruptcy due to the occurrence of certain accidents in the fleet. This phenomenon is rising as several accidents in the maritime environment have been proved to be an initial trigger for massive losses such as iceberg-ship impact case of the Titanic [11], large scale oil spill accident of the Sea Empress [12], death toll in the Sewol’s sinking [13], environmental destruction and species extinction after the Exxon Valdez ran aground and spilled oil [14], Halifax explosion accident in Canada with death estimation reached 2000 people [15,16], and massive financial loss for passenger compensation, ship evacuation and environment restoration in grounding case of the Costa Concordia [17]. From all these, collision and grounding appear to be the highest cause of vessel losses in the category of accidental loads.

Furthermore, from a calculated data of 2018, Allianz [18] showed 90% of global trades/commodities are transported by shipping, and this reflects the contributions of several types of ships to the sustainability of global economy and growth. However, despite its positive value, there are several challenges in its operations. Tables 1 and 2 shows the number of total loses per region from 2008–2017, and Southeast Asia region holds the largest spot, exceeding the East Mediterranean and the Black Sea. Advance assessment in 2017 also pointed out accidental loading was the main cause of largest ships lost as shown in Table 3, with three out of ten largest cases found in Indonesia and Philippines, and observed to have involved bulk carrier and passenger vessels.

Table 1. Review of total losses by top 10 regions: 2008–2017 [18].

Region	Loss Total (ship)
South China, Indochina, Indonesia, and the Philippines	252
East Mediterranean and the Black Sea	169
Japan, Korea, and North China	126
British Isles, North Sea, England Channel and Bay of Biscay	89
Arabian Gulf and approaches	62
West African Coast	51
West Mediterranean	48
East African Coast	34
Russian Arctic and Bering Sea	29
Bay of Bengal	28
Other	241
Total	1129

Table 2. Total losses during 2017 accounting for accident regions [18].

Region	Loss Total	Tendency
South China, Indochina, Indonesia and Philippines	30	↑ 6
East Mediterranean and Black Sea	17	↓ 2
British Isles, North Sea, England Channel and Bay of Biscay	8	=
Arabian Gulf and approaches	6	↑ 3
Japan, Korea, and North China	6	↓ 5
South Atlantic and East Coast of South America	5	↑ 1
West Mediterranean	4	=
West African Coast	3	=
Baltic	2	↑ 2
Bay of Bengal	2	↓ 1
Other	11	↓ 4
Total	94	↓ 4

Table 3. List of the largest ships lost in 2017 [18].

Ship Name	Size (GT)	Accident Date	Description
Stellar Daisy	148431	March 31	Sank after water filled the vessel hull through a crack in approximately 3700 km off the coast of Uruguay
Theresa Arctic	43414	June 2	Grounded on reefs off Kilifi, Kenya
Melite	39964	July 26	Grounded at Pulau Laut, Indonesia
Emerald Star	33205	October 13	Sank off the coast of the Philippines
Maersk Pembroke	31333	August 22	Fire broke out approximately 400 km off the Isles of Scilly.

3. Pioneer Work Related to Impact Loading in the Maritime Environment

The efforts are classified into active and passive major groups as introduced by Törnqvist [19] and Prabowo [20]. The active group is conducting research to support ships during their operations and interactions with other facility and infrastructure in order to avoid accidental phenomena. The navigation system is one the popular field in this group and series of researches are dedicated to improve and expand the capability of radar, communication instrument, gyrocompass, etc, such as the works conducted by Perera and Mo [21], Yoo [22] and An [23]. On the contrary, the passive group focuses on the assessment of structural performance during and after accidents, and the prediction of casualties/loss on the involved parties. However, this work was considered a fundamental aspect in developing marine technology as the results of the assessment and prediction in this group are adopted as reference data for the active group to improve navigation as well as mitigation for ship and other marine structures. Several scholars such as Amdahl [24], Soares [25], Pedersen [26] and Prabowo [27] concentrated their research in this field with varieties of researches, as many as the active group. The main motive of these works was to understand the accidental load/event, such as the reoccurrence of collision, grounding, and explosion despite the achievement of major progress of navigational instruments.

Furthermore, this group was mainly analyzed through the use of numerical analysis (FEM), analytical formula, and empirical approach. The FEM is considered the most developed method compared to others in terms of size, large scale structure, proper ship modeling including the boundary condition, and loading scheme. Moreover, in terms of the considered parameter, more aspects are inputted into the model to idealize the complexity of an accidental model in very specific details. With respect to the works previously mentioned, the analytical formula and empirical approach are currently considered in the analysis as comparison and validation of the numerical calculation.

Similarly, the main motive of this analysis form is that both methods referred to pioneer experimental test with better accuracy as the phenomena were physically investigated.

4. Analysis Preparation and Modelling Configuration

4.1. Vessel Geometry

Two vessels were used in this study with the Ro-Ro used as the struck vessel and cargo as the striking vessel as shown in Figure 2. The struck ship was idealized as a deformable body with an inner structural arrangement such as inner shell, frame, and girder. On the contrary, the striking vessel was defined as a rigid body modelled on bow geometry without inner structure. These assumptions were implemented to focus the damage observation on the struck vessel. Furthermore, by deploying a rigid striking vessel, the worst damage was estimated due to its inability to undergo deformation and cause larger damage than a deformable striking ship.

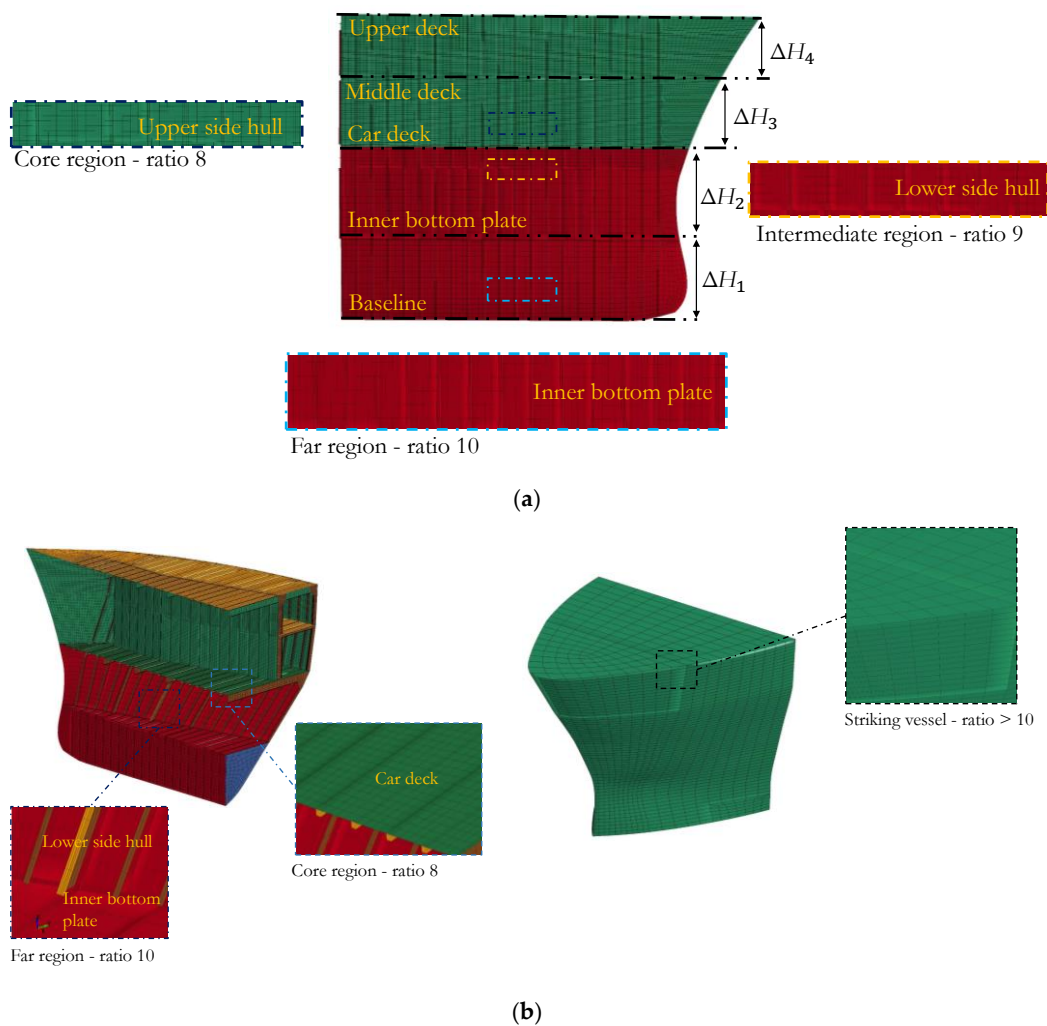


Figure 2. The geometry of the idealized struck vessel: (a) Boxes highlight the mesh configuration on the side hull, and (b) Detail of meshing on the inner structure and the striking vessel.

Based on these configurations, other settings were demanded on the deformable structures to ensure the rupture are well captured. In this case, the discretion of large model was an important task to be conducted, and after several works in the fields of impact engineering and crashworthiness, such as [20,28], the implementation of meshing size based on the ratio of element length and member thickness is proven capable of producing good results. The same strategy was applied in this work with

the finest-smallest mesh of ratio 8 at the core, largest ratio 10 at the far, and ratio 9 at the intermediate region of contact. Moreover, since the striking vessel was modelled as a rigid object, the larger mesh was used to increase the efficiency of the calculation process conducted through nonlinear finite element (NLFE) ANSYS LS-DYNA. Furthermore, the large structures underwent discretization into more than 70,000 element number, and explicit methodology was chosen to calculate configuration due to its effectiveness in estimating the characteristics of impact engineering [29].

4.2. Material Settings

The two vessels were embedded with a material model, and the strain-dependent plastic-kinematic material formulation presented in Equation (1) [29] was applied to idealize the steel properties on the numerical model. The strain-dependent characteristic was considered because of its relation to the rupture criterion. Furthermore, as described in the previous discussion, immense structural damage is one of the casualty forms mostly observed during and after the occurrence of an accidental load. Therefore, it was necessary to define a condition when the material could be considered to have fail or ruptured and for the purpose of this study, a rupture value of 0.2 was selected. Besides failure, the Cowper–Symonds values were also defined on the material as its nonlinearity was expected since the analysis has the ability to make the material surpass yield point, therefore, value $C = 3200/s$ and $P = 0$ were applied on the mathematical expression. However, when compared with mild steel, the value in this work is higher considering the material type selected, high-strength low-alloy (HSLA) steel (yield stress $\sigma_Y = 440$ MPa, density $\rho = 7850$ kg/mm, Poisson ratio $\nu = 0.3$, hardening parameter $n = 0$ and elastic modulus $E = 210,000$ MPa), and effect of the impact to material behaviour.

$$\sigma_Y = \left[1 + \left(\frac{\dot{\epsilon}}{C} \right)^{\frac{1}{P}} \right] (\sigma_0 + \beta E_P \epsilon_p^{eff}) \quad (1)$$

where σ_Y is the yield stress, $\dot{\epsilon}$ is the strain rate, C and P are the Cowper–Symonds strain rate parameters, σ_0 is the initial yield stress, β is the hardening parameter, E_P is the plastic-hardening modulus, E is the elastic modulus, and ϵ_p^{eff} is the effective plastic strain.

4.3. Boundary Conditions

The accidental load was defined as the collision between two vessels with the striking vessel hitting the designated target on the struck vessel's side shell. Specifically, the target was placed on the car deck of the Ro-Ro below the upper and middle decks. However, in order to investigate several structural performances of the card deck, different collision angles, 60° , 90° , and 120° , were applied on the scenario configuration according to the Cartesian coordinate system. Even though the 60° and 120° are actually the same degrees in different quadrants, different results were expected due to the curve geometry of the struck vessel. The collision geometry of the NLFE analysis is presented in Figure 3.

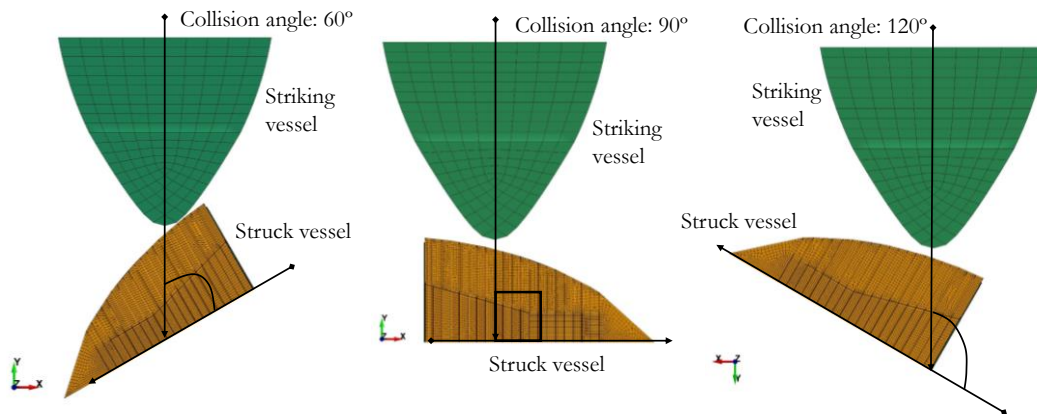


Figure 3. A variety of collision angle applied to the scenarios.

During vessel collision, the striking speed applied was 12 knots or approximately 6 m/s with restrained rotational displacements. The struck vessel was made constant (not moving) with the fixation attached on the edge of decks, inner bottom plate, and side transverse frame. Moreover, since collision is the main subject of this study, contact, involving frictions, is an inevitable phenomenon. Therefore, automatic contact surface-to-surface model was used to idealize the interaction of surface geometry between the struck and striking vessel, and the values of friction coefficient were set at $\mu_k = 0.57$ and $\mu_s = 0.74$ for kinematic and static values respectively.

5. Structural Assessments

5.1. Internal Energy

The structural assessment of the struck vessel was first conducted by observing behaviours of the internal energy, which was included in the crashworthiness criteria. The graph below illustrates the numbers of structural members destroyed on impact as well as the level of the expected damage. Figure 4 shows the collision angle 60° to have produced the highest energy level, followed by 120° and 90°, consecutively. The results also indicated that the destruction of the struck vessel in oblique collision 60° lasts longer, which may be important background regarding high energy pattern. Through the representation of the internal energy at the end of the collision a shown in Figure 5, a parabolic shape was produced when the collision angle was in its vertex or lowest point.

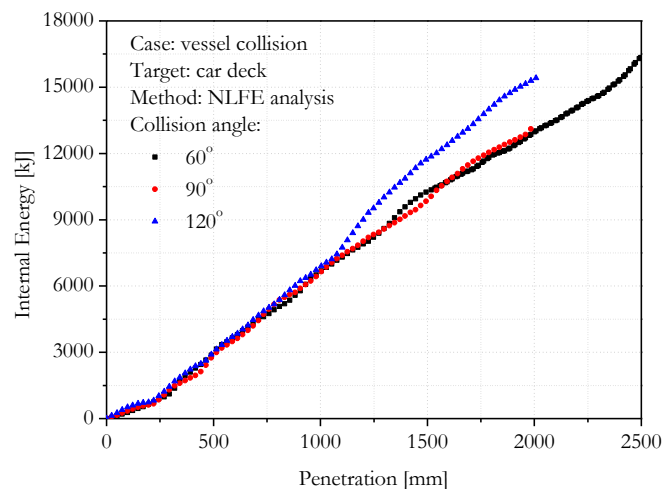


Figure 4. Summary of the internal energy based on the proposed cases.

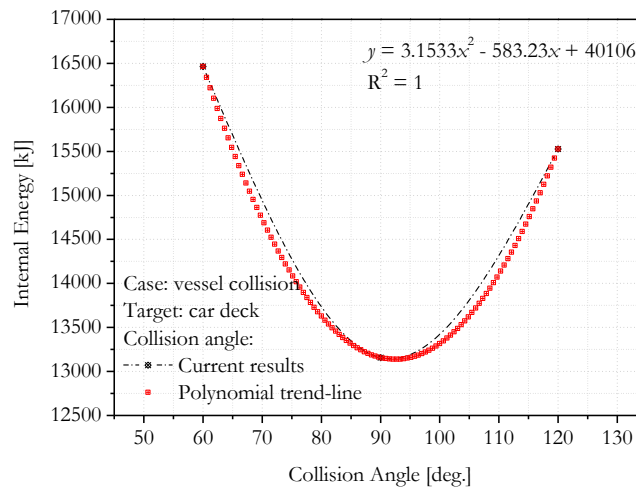


Figure 5. Pattern of the internal energy on a variety of collision angle.

This phenomenon suggested that during side collision, the side hull is more prone to oblique collision than a perpendicular one or perfect T-collision. This statement is founded on the less energy observed in the angle 90°, which shows that less damaged structure occurred after the collision process.

5.2. Energy Ratio

This is the proportion of the total energy in a system to the initial energy, as shown in the mathematical expressions in Equations 2 and 3. However, if the left-hand side falls below the right hand, it is possible to conclude that energy is being absorbed artificially, perhaps by an hour-glassing phenomenon, which may occur due to major damage of the idealized structures. This fundamental calculation was matched with the results in Figure 6 where the ratio was found not to be perfectly one since some energy was affected by an hourglass. However, a very satisfying condition was indicated as the final results for all cases exceed 95%, and the hourglass proportion less than 5%. A more specific discussion on hourglass is presented in the next sub-section.

$$E_{kin} + E_{int} + E_{si} + E_{rw} + E_{damp} + E_{hg} = E_{kin}^0 + E_{int}^0 + W_{ext} \tag{2}$$

$$E_{ratio} = \frac{E_{total}}{E_{total}^0 + W_{ext}} \tag{3}$$

where E_{kin} is the current kinetic energy, E_{int} is the current internal energy, E_{si} is the current sliding interference energy (including friction), E_{rw} is the current rigid wall energy, E_{damp} is the current damping energy, E_{hg} is the current hourglass energy, E_{kin}^0 is the initial kinetic energy, E_{int}^0 is the initial internal energy, W_{ext} is the external work, E_{ratio} is the energy ratio, and E_{total}^0 is the initial total energy.

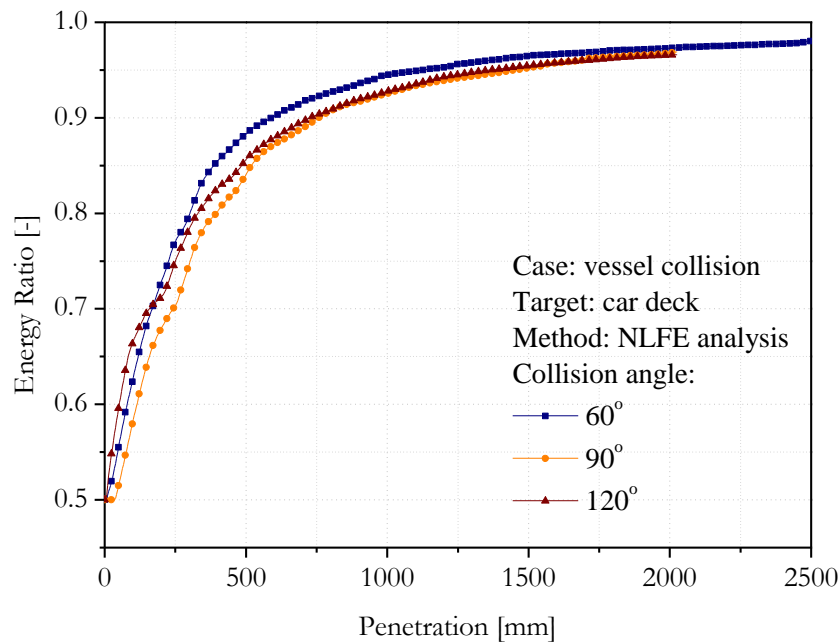


Figure 6. Ratio of the internal energy to the kinetic energy during collisions.

5.3. Hourglass Phenomenon

Hourglass is a behaviour of a numerical model to be deformed in non-physical ways or geometrically due to the excessive artificially applied load. As initially predicted in the discussion of the energy ratio, a very small part of the energy was artificially absorbed by hourglass and the results presented in Figures 7–9 show compatibility with the prediction, even though it is minor.

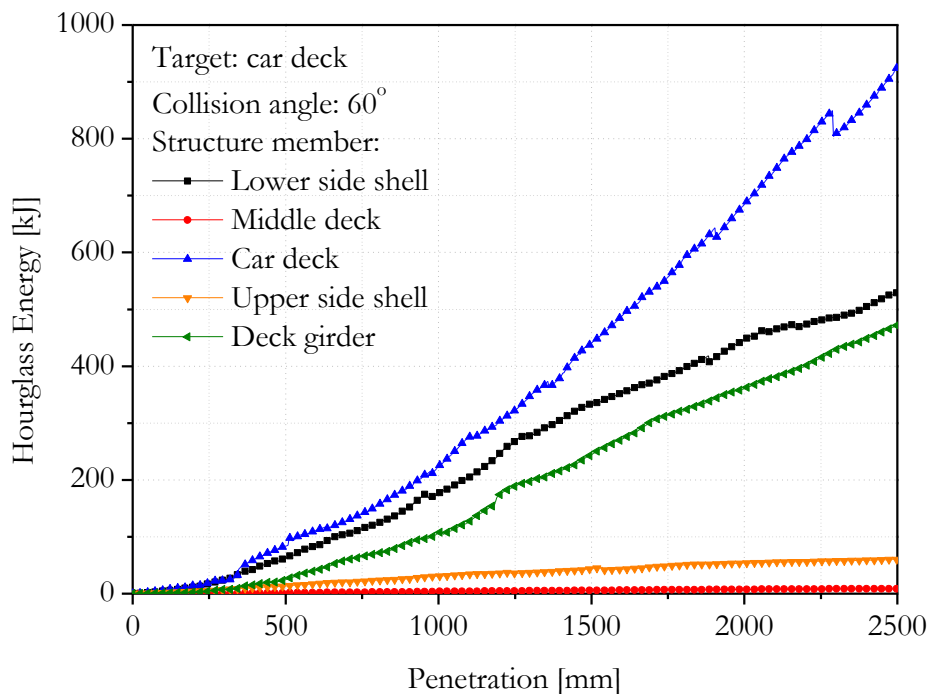


Figure 7. Hourglass energy of the collision angle 60°.

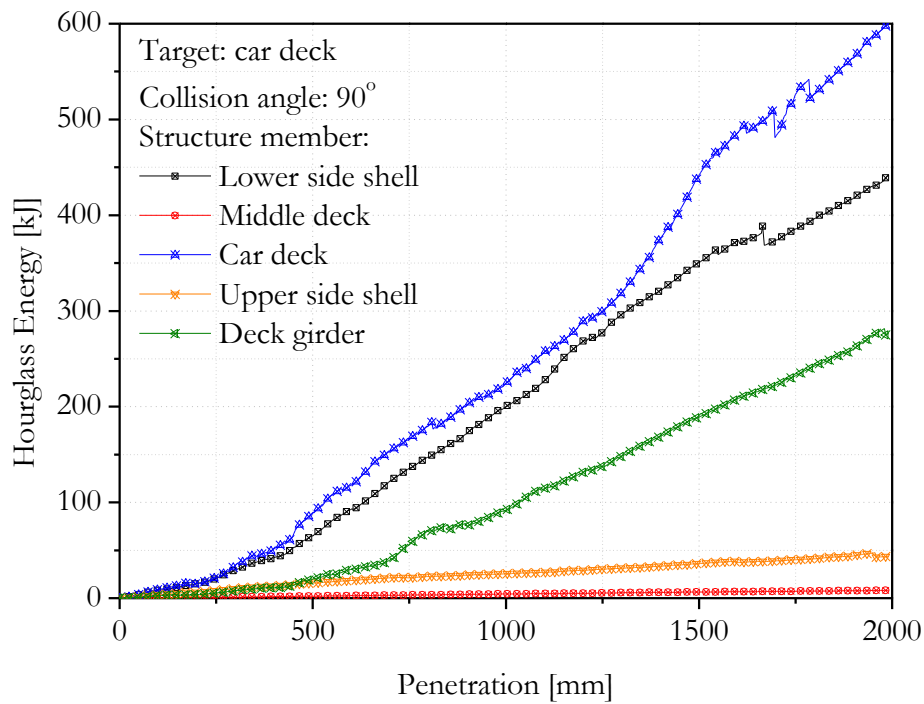


Figure 8. Hourglass energy of the collision angle 90°.

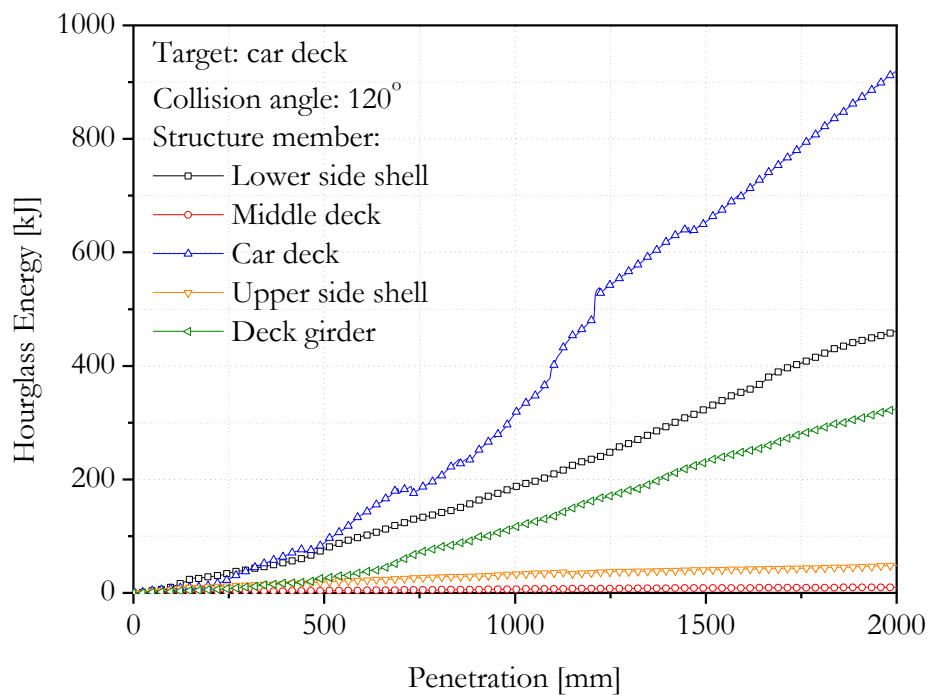


Figure 9. Hourglass energy of the collision angle 120°.

The summary of the designed collision cases indicated the T-collision shown in Figure 8 to have produced the lowest hourglass energy compared to the oblique cases in Figures 7 and 9. However, a detail observation has the ability to identify the most contributing member in the hourglass phenomenon. Furthermore, the tendency of the car deck was observed to have produced the highest level, followed by the lower side hull, deck girder, upper side, and middle decks, respectively. It was especially found that the upper side and middle decks have extremely low hourglass with approximation in the range of 0–50 kJ. Moreover, associating the result of this subsection with the expected damage pattern after vessel collision showed a higher level of damage is experienced by a

member during impact and the possibility of hourglass occurrence increase for this member. However, this leads to a very low energy value with no effect on the reliability of the present calculation. Therefore, there is need to consider an alternative to fully neutralize the hourglass in very high dynamic and nonlinear simulation and this can be achieved through the development of a fully integrated element formulation in the deformable body as conducted in [30–32].

5.4. Rupture Strain

As defined in the numerical configuration, rupture is experienced by a material when the ultimate strain is exceeded due to accidental load. In case of the vessel collisions, the strain distribution on the struck vessel reached a quite long extent in oblique collisions of 60° and 120° as shown in Figures 10 and 11. The strain observed indicated that the earlier contact of the side part of the striking vessel and struck vessel occurred before the tip of the striking vessel hit the target. This pattern is very different compared to the T-collision, as shown in Figure 12. This illustration showed the opening on the struck vessel was perfect with the tip of the striking vessel which penetrated the target straight to the transverse direction. Therefore, due to more local damage on the struck vessel, the internal energy and hourglass for angle 90° were lower than the oblique cases.

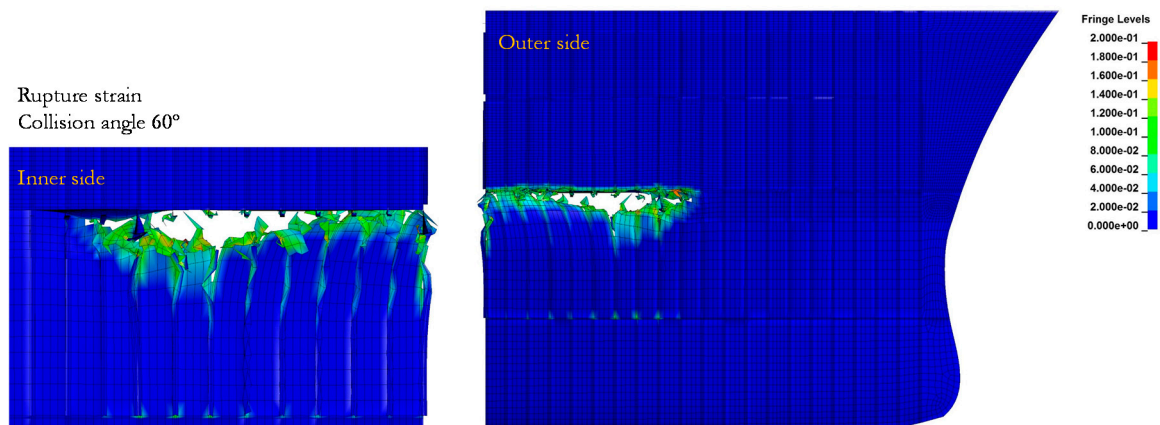


Figure 10. Contours of the strain near the car deck: Angle 60°.

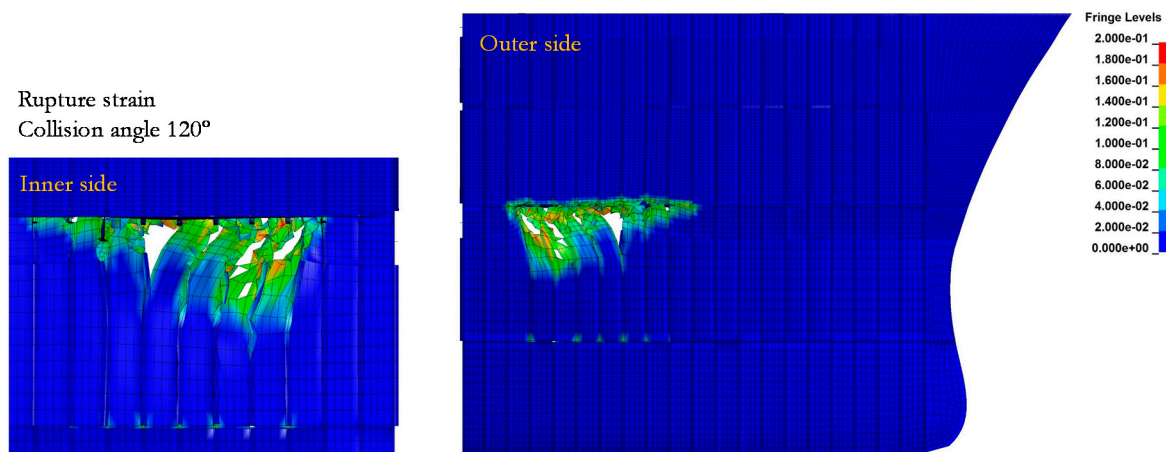


Figure 11. Contours of the strain near the car deck: Angle 120°.

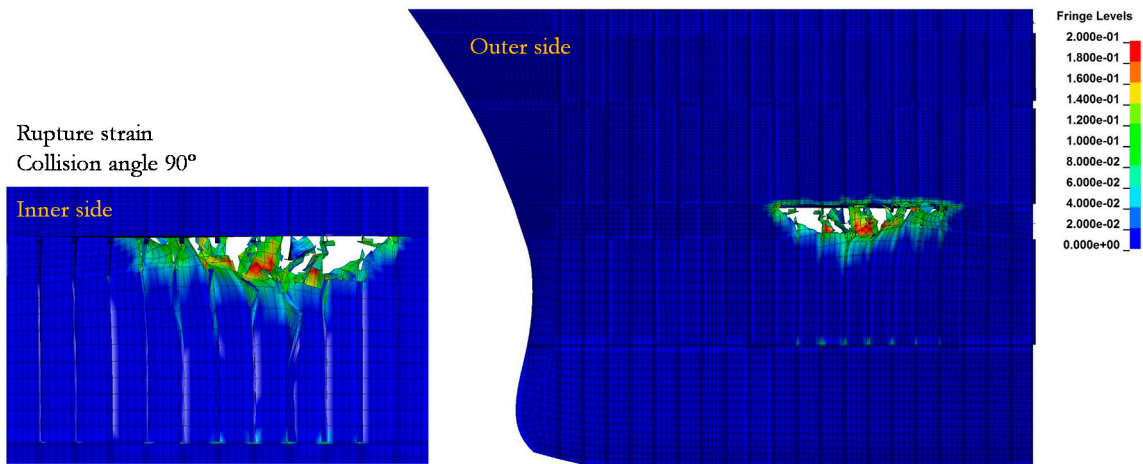


Figure 12. Contours of the strain near the car deck: Angle 90°.

The observation of the damage pattern showed the most side frame on the oblique collision 120° was folded on the lower part while the upper part was crushed and pushed on the direction of the striking angle. Furthermore, the curved geometry on the fore-peak section made the crushing pattern of two oblique collisions different even though the angle size is the same according to the Cartesian diagram. In terms of the damage extent, the collision in 60° caused longer tear on the connection of the car deck and lower side shell influenced by deeper penetration. Moreover, the calculation of the penetration in the same depth predicted the damage length to be similar in terms of size.

5.5. Critical Stress

The stress in the current structural assessment was conducted to investigate the total number of members affected due to the car deck. According to the critical stress presented by von-Mises formulation in Figures 13–15, the affected members for the three cases were similar, and they include car deck (main target), girder, lower hull, upper hull, and middle deck. However, despite these similarities, high-stress intensity occurred quite extensive on the lower hull of the collision case 90°. It is, therefore, possible to come up with the estimation that the collision would continue, and the part covered by high stress would experience the earliest rupture, and the element removed in the calculation. It was also noted that the oblique collisions and T-collision have a quite distinct extent in terms of damage and stress with the former having the tendency to form an incision rather than deep-focus penetration produced by the latter on the struck vessel.

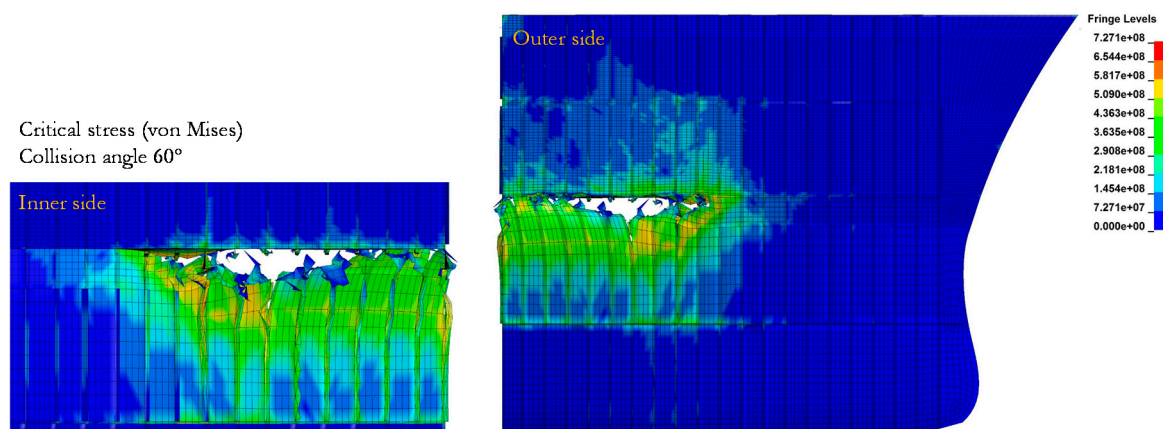


Figure 13. Critical stress (von Mises formulation) of the collision Angle 60°.

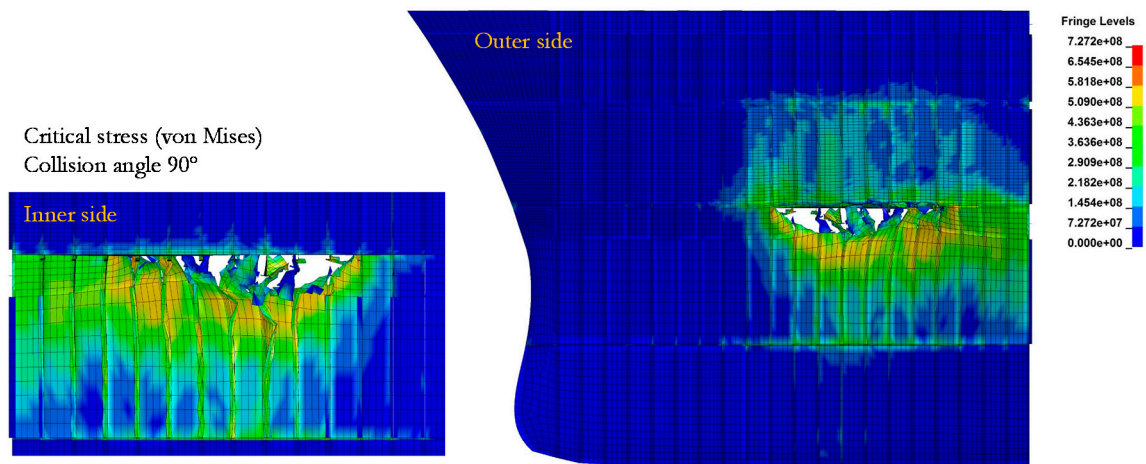


Figure 14. Critical stress (von Mises formulation) of the collision angle 90°.

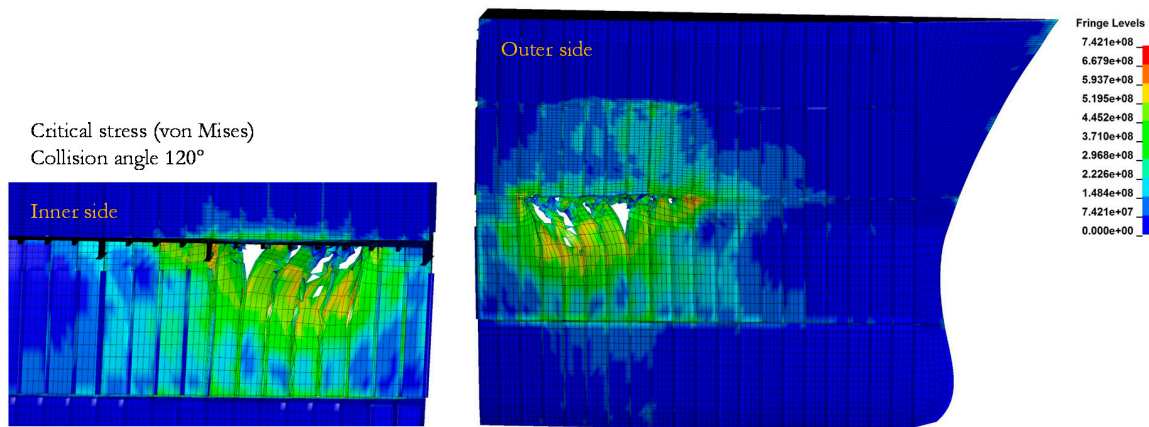


Figure 15. Critical stress (von Mises formulation) of the collision angle 120°.

The inflicted damage due to a variety of penetration styles influenced the stress contour on the side hull. Moreover, the oblique collisions in Figures 13 and 15 caused stress distribution to the longitudinal direction of the struck vessel, while the T-collision in Figure 14 caused high-stress intensity on the lower part of the hull opening which was explicitly distributed on the lower side hull, including its local components, such as shell and frame. This condition indicated the hull part was in a critical state before the larger tearing occurred and a deeper penetration was expected to lead to the same pattern on the side hull. A similar case is found on the 120° collision angle with the red contours spotted on the connection between the car deck and side hull. However, this spot was not a complete failure during an interaction between two ships, and the stress was intact at the end of the collision process. Therefore, the tearing length may reach this spot if a larger part of the striking bow penetrates the struck ship on impact.

6. Conclusions

This research was dedicated to investigating structural responses of the Ro-Ro vessel during a series of accidental load designed using a vessel-to-vessel collision with the angle varied in the calculation, and the analysis was conducted through the use of nonlinear finite element (NLFE) analysis. The results obtained indicated internal energy of the oblique collision case to be superior to the T-collision case, and this was verified by observing the damage level of the rupture strain and critical stress. Moreover, more local damage was produced in the T-collision case, which caused fewer casualties on the struck vessel. Besides physical behaviour, verification of the calculation process of the

current work was also conducted by investigating energy ratio, and a very small portion of the energy was found to have been absorbed artificially.

Hourglass phenomenon was expected, and higher damaged members in the simulation were found to have the capability to produce higher hourglass possibility. Therefore, these findings showed energy ratio and hourglass energy to be important criteria, especially in the structural assessment of accidental load in the maritime environment, and they are recommended to be included as validation criteria in NLFE calculation considering that accidental load causes high nonlinearities. However, implementation of the current method and verification are also viable to be used in any assessment related to impact or accidental load on structures. Therefore, future work in this field should extend collision investigation by involving other angles and conduct a comparative study with a head-to-head collision case. It should also provide a concise and precise description of the experimental results, interpretation as well as the experimental conclusions to be drawn.

Author Contributions: All the authors contributed equally to the paper's preparation.

Funding: This research was an independent project without grant funding based on the collaboration of Laboratory of Design and Computational Mechanics, Universitas Sebelas Maret, Indonesia and Laboratory of Ship Structure and Vibration Analysis, Pukyong National University, South Korea.

Conflicts of Interest: The authors declare no conflict of interest.

References

1. Rusli, M.H.M. *Maritime Highways of Southeast Asia: Alternative Straits?* RSIS Commentaries, Nanyang Technological University: Singapore, 2012.
2. ERIA. Sea lane security in the selected EAS countries. In *Sea Lane Security of Oil and Liquefied Natural Gas in the EAS Region*; ERIA Research Project Report 2015-14; Kimura, S., Morikawa, T., Singh, S., Eds.; ERIA: Jakarta, Indonesia, 2016; pp. 41–55.
3. Prabowo, A.R.; Bae, D.M.; Cho, J.H.; Sohn, J.M. Analysis of structural crashworthiness and estimating safety limit accounting for ship collisions on strait territory. *Lat. Am. J. Sol. Struct.* **2017**, *14*, 1594–1613. [[CrossRef](#)]
4. ASDP. Map (Trajectories). ASDP Indonesia Ferry, Jakarta. 2019. Available online: <https://www.indonesiaferry.co.id/en/komersil> (accessed on 17 February 2019).
5. Allianz. *Safety and Shipping Review 2017*; Allianz Global Corporate and Specialty: Munich, Germany, 2017.
6. Geffroy, A.G.; Longère, P.; Leblé, B. Fracture analysis and constitutive modelling of ship structure steel behaviour regarding explosion. *Eng. Fail. Anal.* **2011**, *18*, 670–681. [[CrossRef](#)]
7. Prabowo, A.R.; Muttaqie, T.; Sohn, J.M.; Harsritanto, B.I.R. Investigation on structural component behaviours of double bottom arrangement under grounding accidents. *Theor. Appl. Mech. Lett.* **2019**, *9*, 50–59. [[CrossRef](#)]
8. Kujala, P.; Goerlandt, F.; Way, B.; Smith, D.; Yang, M.; Khan, F.; Veitch, B. Review of risk-based design for ice-class ships. *Mar. Struct.* **2019**, *63*, 181–195. [[CrossRef](#)]
9. Prabowo, A.R.; Bae, D.M.; Sohn, J.M.; Zakki, A.F.; Cao, B.; Wang, Q. Analysis of structural damage on the struck ship under side collision scenario. *Alex. Eng. J.* **2018**, *57*, 1761–1771. [[CrossRef](#)]
10. Babicz, J. *Wärtsilä, Encyclopedia of Ship Technology*; Wärtsilä Corporation: Helsinki, Finland, 2015.
11. Labib, A.; Read, M. Not just rearranging the deckchairs on the Titanic: Learning from failures through Risk and Reliability Analysis. *Saf. Sci.* **2013**, *51*, 397–413. [[CrossRef](#)]
12. Law, R.J. Chapter 35—The Sea Empress Oil Spill, 1996. In *Oil Spill Science and Technology*; Gulf Professional Publishing: Cambridge, MA, USA, 2011; pp. 1109–1117.
13. Park, S.H.; Pham, T.Y.; Yeo, G.T. The Impact of ferry disasters on operational efficiency of the South Korean Coastal Ferry Industry: A DEA-Window Analysis. *Asian J. Shipp. Logist.* **2018**, *34*, 248–255. [[CrossRef](#)]
14. Morris, B.F.; Loughlin, T.R. Chapter 1—Overview of the Exxon Valdez Oil Spill 1989–1992. In *Marine Mammals and the Exxon Valdez*; Elsevier: Amsterdam, The Netherlands, 1994; pp. 1–22.
15. Carter, P.L. The Halifax Explosion a century later: Lessons for our time. *Am. J. Surg.* **2018**, *215*, 772–774. [[CrossRef](#)] [[PubMed](#)]
16. Amyotte, P.R. Some myths and realities about dust explosions. *Proc. Saf. Environ. Prot.* **2014**, *92*, 292–299. [[CrossRef](#)]

17. Giustiniano, L.; Cunha, M.P.E.; Clegg, S. The dark side of organizational improvisation: Lessons from the sinking of Costa Concordia. *Bus. Horiz.* **2016**, *59*, 223–232. [[CrossRef](#)]
18. Allianz. *Safety and Shipping Review 2018*; Allianz Global Corporate and Specialty: Munich, Germany, 2018.
19. Törnqvist, R. *Design of Crashworthy Ship Structures*; Technical University of Denmark: Lyngby, Denmark, 2003.
20. Prabowo, A.R. *Crashworthiness Assessment of Ship Structures under Collision and Grounding*; Pukyong National University: Busan, Korea, 2018.
21. Perera, L.P.; Mo, B. Ship performance and navigation data compression and communication under autoencoder system architecture. *J. Ocean Eng. Sci.* **2018**, *3*, 133–143. [[CrossRef](#)]
22. Yoo, S.L. Near-miss density map for safe navigation of ships. *Ocean Eng.* **2018**, *163*, 15–21. [[CrossRef](#)]
23. An, K. E-navigation services for Non-SOLAS ships. *Int. J. e-Navig. Mar. Econ.* **2016**, *4*, 13–22. [[CrossRef](#)]
24. Moan, T.; Amdahl, J.; Ersdal, G. Assessment of ship impact risk to offshore structures—New NORSOK N-003 guidelines. *Mar. Struct.* **2019**, *63*, 480–494. [[CrossRef](#)]
25. Chen, B.Q.; Liu, B.; Soares, C.G. Experimental and numerical investigation on the influence of stiffeners on the crushing resistance of web girders in ship grounding. *Mar. Struct.* **2019**, *63*, 351–363. [[CrossRef](#)]
26. Liu, B.; Pedersen, P.T.; Zhu, L.; Zhang, S. Review of experiments and calculation procedures for ship collision and grounding damage. *Mar. Struct.* **2018**, *59*, 105–121. [[CrossRef](#)]
27. Prabowo, A.R.; Muttaqie, T.; Sohn, J.M.; Bae, D.M. Nonlinear analysis of inter-island RoRo under impact: Effects of selected collision's parameters on the crashworthy double-side structures. *J. Braz. Soc. Mech. Sci. Eng.* **2018**, *40*, 248. [[CrossRef](#)]
28. Alsos, H.S.; Amdahl, J. On the resistance of tanker bottom structures during stranding. *Mar. Struct.* **2007**, *20*, 218–237. [[CrossRef](#)]
29. ANSYS. *ANSYS LS-DYNA User's Guide*; ANSYS, Inc.: Canonsburg, PA, USA, 2019.
30. ANSYS. *ANSYS Mechanical APDL Element Reference*; ANSYS, Inc.: Canonsburg, PA, USA, 2019.
31. Prabowo, A.R.; Cho, H.J.; Byeon, J.H.; Bae, D.M.; Sohn, J.M. Investigation of impact phenomena on the marine structures: Part I—On the behaviour of thin-walled double bottom tanker during rock-structure interaction. *IOP Conf. Ser. J. Phys. Conf. Ser.* **2017**, *953*, 012003. [[CrossRef](#)]
32. Prabowo, A.R.; Sohn, J.M.; Bae, D.M.; Harsritanto, B.I.R. Crashworthiness assessment of double-hull tanker structures under ship grounding actions. *MATEC Web Conf.* **2018**, *195*, 04008. [[CrossRef](#)]



© 2019 by the authors. Licensee MDPI, Basel, Switzerland. This article is an open access article distributed under the terms and conditions of the Creative Commons Attribution (CC BY) license (<http://creativecommons.org/licenses/by/4.0/>).